

Article

Vehicle–Grid Interaction Pricing Optimization Considering Travel Probability and Battery Degradation to Minimize Community Peak–Valley Load

Kun Wang ¹, Yalun Li ^{2,*}, Chaojie Xu ³, Peng Guo ⁴, Zhenlin Wu ⁴ and Jiuyu Du ¹

¹ School of Vehicle and Mobility, Tsinghua University, Beijing 100084, China; wangkun.26@outlook.com (K.W.); dujiuyu@tsinghua.edu.cn (J.D.)

² Department of Electrical Engineering, Tsinghua University, Beijing 100084, China

³ School of Mechanical Engineering, University of Shanghai for Science and Technology, Shanghai 200093, China; 203601726@st.usst.edu.cn

⁴ Shanghai Qiyuan Green Power Technology Co., Ltd., Shanghai 201702, China; guopeng@cpirhzl.com (P.G.); wuzhenlin@cpirhzl.com (Z.W.)

* Correspondence: liyalun@tsinghua.edu.cn

Abstract: Vehicle-to-Grid (V2G) technology has been widely applied in recent years. Under the time-of-use pricing, users independently decide the charging and discharging behavior to maximize economic benefits, charging during low-price periods, discharging during high-electricity periods, and avoiding battery degradation. However, such behavior under inappropriate electricity prices can deviate from the grid's goal of minimizing peak–valley load difference. Based on the basic electricity data of a community in Beijing and electricity vehicle (EV) random travel behavior obtained through Monte Carlo simulation, this study establishes a user optimal decision model that is influenced by battery degradation and electricity costs considering depth of discharge, charging rate, and charging energy loss. A mixed-integer linear programming algorithm with the objective of minimizing the cost of EV users is constructed to offer the participation power of V2G. By analyzing grid load fluctuations under different electricity pricing strategies, the study derives the formulation and adjustment rules for optimal electricity pricing that achieve ideal load stabilization. Under 30% V2G participation, the relative fluctuation of grid load is reduced from 31.81% to 5.19%. This study addresses the challenge of obtaining optimal electricity prices to guide users to participate in V2G to minimize the peak–valley load fluctuation.



Academic Editor: Pascal Venet

Received: 12 January 2025

Revised: 12 February 2025

Accepted: 14 February 2025

Published: 16 February 2025

Citation: Wang, K.; Li, Y.; Xu, C.; Guo, P.; Wu, Z.; Du, J. Vehicle–Grid Interaction Pricing Optimization Considering Travel Probability and Battery Degradation to Minimize Community Peak–Valley Load. *Batteries* **2025**, *11*, 79. <https://doi.org/10.3390/batteries11020079>

Copyright: © 2025 by the authors. Licensee MDPI, Basel, Switzerland. This article is an open access article distributed under the terms and conditions of the Creative Commons Attribution (CC BY) license (<https://creativecommons.org/licenses/by/4.0/>).

1. Introduction

Fluctuations in grid load, especially the mismatch with renewable energy, pose significant challenges to the stability of the power system [1]. With the rapid adoption of electric passenger vehicles (EVs), buses [2] and trucks [3], the demand for vehicle charging has increased. Different charging modes can lead to varying degrees of growth in grid load peaks, posing difficulties for the operation of the power grid [4]. Additionally, the large-scale integration of renewable energy, due to the dynamic fluctuations in generation and load, may also lead to grid instability [5,6]. Amid the advancement of smart grids, uni-directional orderly charging (V1G) and Vehicle-to-Grid (V2G) technology are increasingly becoming important solutions for minimizing grid peak–valley loads fluctuations. V1G refers to the use of intelligent control measures to optimize EVs' charging time and power

under the premise of meeting their charging demand, and it is already compatible with the commercial electric vehicle supply equipment (EVSE) and EVs and implies limited concerns on battery lifespan loss. Correspondingly, V2G allows EVs to charge then feed excess electricity back into the grid when they are not in travel, thereby achieving peak shaving and valley filling for the grid [7]. In our previous research work [8], we quantitatively compared the potential of V1G and V2G in reducing grid load fluctuations. V2G offers a clear advantage over V1G due to its potential for grid peak shaving. This is particularly evident in that V2G with a participation of 40% causes a lower load range than that of 100% orderly charging.

Under the time-of-use (TOU) pricing, users can independently decide the charging and discharging behavior of their EVs. They can charge their vehicles when electricity price is low and discharge them when price is high, thereby achieving peak–valley price arbitrage [9]. However, such behavior under inappropriate electricity prices will result in greater fluctuations in grid load. As the proportion of users participating in V2G increases, the original load valleys may turn into peaks, and the peaks may turn into valleys [10]. The batteries of EVs face degradation during charging and discharging. In the process of participating in V2G, the high-frequency energy exchanges between EVs and the grid can accelerate the battery degradation process [11]. After accounting for the cost losses caused by battery degradation during charging and discharging, users' willingness for arbitrage behavior is decreased, resulting in a complex charging load to the distribution grid. Therefore, the method to achieve an ideal charging load to the grid necessitates in-depth research [12].

Battery degradation is a core element considered in the V2G decision. There are studies on battery degradation behavior under V2G currently. Research by Dubarry et al. [13] shows that EVs participating in V2G once per day experience over 33% more degradation compared to EVs under regular driving conditions. It is generally believed that V2G operating conditions with smaller SOC variations, such as frequency regulation or mild peak shaving, have a relatively small impact on battery aging [14]. However, Jafari et al. [15] argue that under the same Ah throughput, frequency regulation leads to greater capacity degradation compared to peak shaving. Carmeli et al. [16] reached similar conclusions, showing that while the Ah throughput nearly doubled from 120,000 Ah to 230,000 Ah, the battery lifespan was reduced by only 20%. Li et al. [17] illustrated that excessive fast charging of batteries can result in unexpected battery accidents. Empirical models often simplify battery degradation as a function of energy or power throughput [18]. Liu et al. [19] developed an empirical aging model for lithium-ion batteries that incorporates state of charge (SOC) and depth of discharge (DoD) and established a minimum-cost model for orderly electricity usage that takes battery degradation into account. Zhang et al. [20] investigated the main factors contributing to capacity degradation during battery discharge and, considering the power control characteristics of EV discharging, developed a battery cycle life degradation model that accounts for DoD and discharge intervals. Todeschini et al. [21], while neglecting the impact of temperature, established a linear relationship between battery degradation and SOC, proposing a semi-empirical formula model that incorporates both C-rate and SOC. In recent studies, the development of protective layers for electrodes has been shown to reduce degradation effects in various types of batteries. For example, research by Guo et al. [22] has shown that the use of a fast ion conductor protective layer can stabilize the zinc metal anode in zinc-based batteries, enhancing performance stability and preventing dendrite growth. Similarly, the advancements in 3D electrodes for vanadium redox flow batteries, discussed by Ye et al. [23], demonstrate that the integration of three-dimensional structures improves ion transport and battery lifespan by enhancing the electrode's electrochemical activity and structural stability. These findings suggest that

protective layers and advanced electrode structures can also play a critical role in mitigating battery degradation in V2G applications.

When coordinating the EV users to achieve an ideal charging load in V2G, TOU electricity price is a decisive factor to guide the charging behavior. The pricing strategy under V2G follows a certain pattern, typically showing a positive correlation with the grid load. When the grid load is low, electricity prices are generally lower, and when the grid load is high, electricity prices increase [24]. This pricing mechanism encourages users to charge their vehicles during valley periods and discharge energy back to the grid during peak load periods, thereby narrowing the range of grid load fluctuations [25]. During the same time period, an increase in electricity prices raises users' willingness to discharge, prompting some users to shift their decision from charging to discharging [26]. Conversely, a decrease in electricity prices enhances users' willingness to charge and reduces their willingness to discharge.

Studies in the literature [27–30] have explored the bidirectional dynamic evolution process of V2G based on game theory, dynamic games, and evolutionary games, demonstrating that both parties can benefit from the interaction only when electricity prices are controlled within a certain range. Wu et al. [31] developed a strategy optimization model that comprehensively considers EV participation in V2G interactions, incorporating factors such as user willingness to participate, travel demands, and the electricity market, as well as the participation intentions of various market stakeholders.

Although existing research has made some progress in areas such as battery degradation under V2G, interaction decision-making between EVs and the grid, and electricity pricing strategies, the way in which electricity pricing incentivizes user participation in V2G and stabilizes grid load remains to be further clarified. On this basis, it is necessary to propose an optimal strategy for the formulation and adjustment of electricity prices. The objective of users participating in V2G arbitrage is to obtain maximal profits, while the grid's objective is to achieve load stabilization [32]. In the V2G arbitrage scenario established in this paper, users make charging and discharging decisions to minimize total costs (or maximize total revenue) under the premise of meeting their travel needs. These decisions take into account electricity expenses, battery degradation, and loss costs arising from the grid due to battery polarization and power variation. Subsequently, by adjusting the predefined electricity prices, users are guided to alter their charging and discharging strategies. This approach not only enables users to pursue arbitrage opportunities but also stabilizes the grid load, thereby achieving a coordinated balance of interests between users and the grid. Ultimately, an optimal electricity pricing strategy is obtained.

The main contributions of this work can be summarized as follows:

1. A multi-parameter coupled quantitative model for battery degradation cost and energy loss cost due to the battery polarization and power fluctuation has been established, which will accompany users' charging and discharging behaviors.
2. A price formulation and adjustment strategy to guide users' charging and discharging decisions aimed at reducing grid load fluctuations is proposed under the community scenario. Its effectiveness in stabilizing grid load is validated. Additionally, the charging demands of EV clusters are analyzed to reveal patterns that can influence electricity price adjustments.
3. The impact of extended battery life and increased V2G participation ratio on grid load is investigated. Furthermore, the effectiveness of the proposed price formulation and adjustment strategy in addressing these changes is validated.

The rest of this paper is organized as follows. Section 2 presents the proposed methodology and optimization algorithm, including Monte Carlo simulation of EV random charging, V2G cost models, electricity price strategy and the optimization algorithm. Section 3 describes the analysis results. Optimized load and electricity price under additional scenarios are further discussed in Section 4. Finally, conclusions are discussed in Section 5.

2. Proposed Methodology and Optimization Algorithm

Figure 1 illustrates the analysis framework of this study. The inputs to the global optimization model include Monte Carlo simulation results of EV random charging, a battery degradation and energy loss model, and a predefined electricity pricing scheme. By constraining EVs' power and energy changes, the optimization objective function is to maximize the economic profits of users participating in V2G after deducting various costs under the formulated electricity price. Subsequently, the grid load results under users engaging in charging and discharging arbitrage behavior are obtained, and the electricity price is adjusted according to the fluctuation of grid load to guide users to change their charging and discharging decisions, achieving a more stabilized grid load. Ultimately, the optimal electricity price is derived.

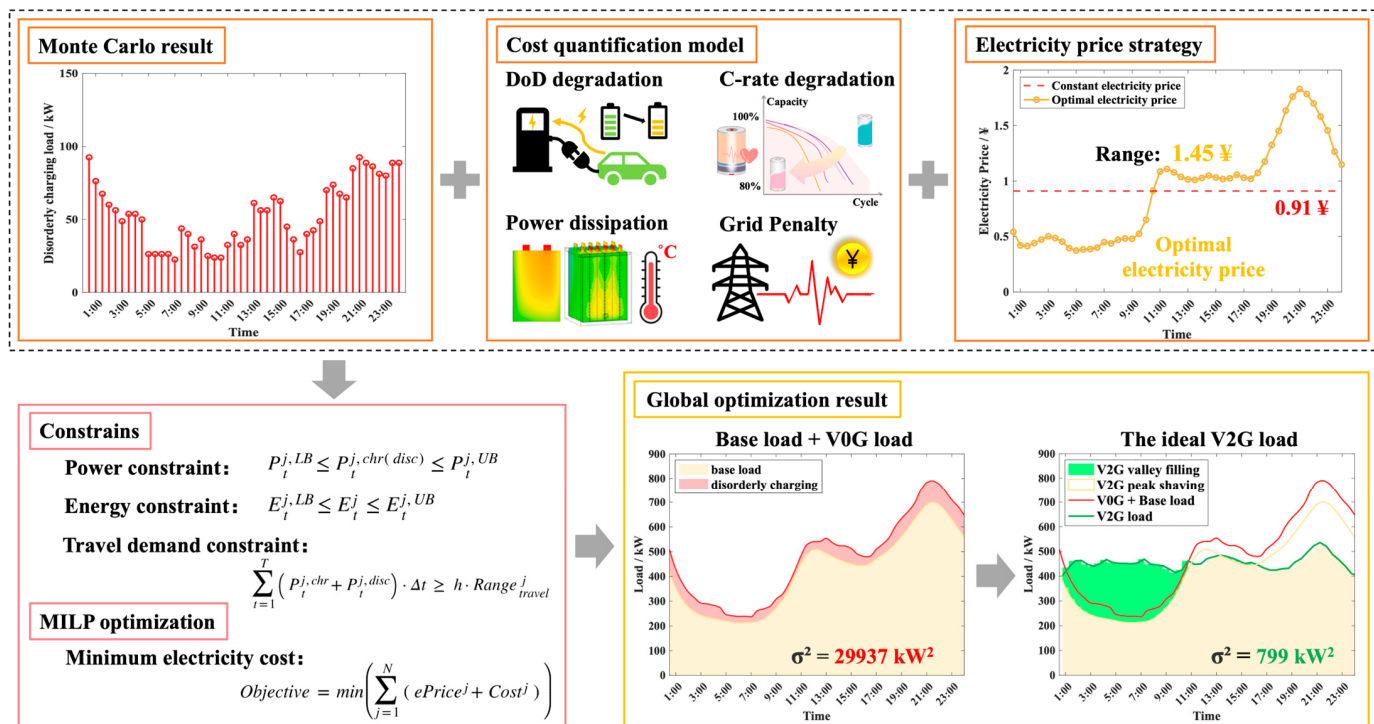


Figure 1. V2G research framework based on EVs and grid decisions.

2.1. Simulation of Random Charging and EV Travel Characteristics

The travel characteristics of EVs, such as the initial SOC distribution, travel distance distribution, etc., are obtained according to the Beijing Transport Development Annual Report [33], as shown in Figure 2. Figure 2a shows the state of charge (SOC) at the start of EV travel, while Figure 2b illustrates the distribution of travel range. The distribution of travel start times is presented in Figure 2c, and Figure 2d displays the number of EVs in transit throughout the day.

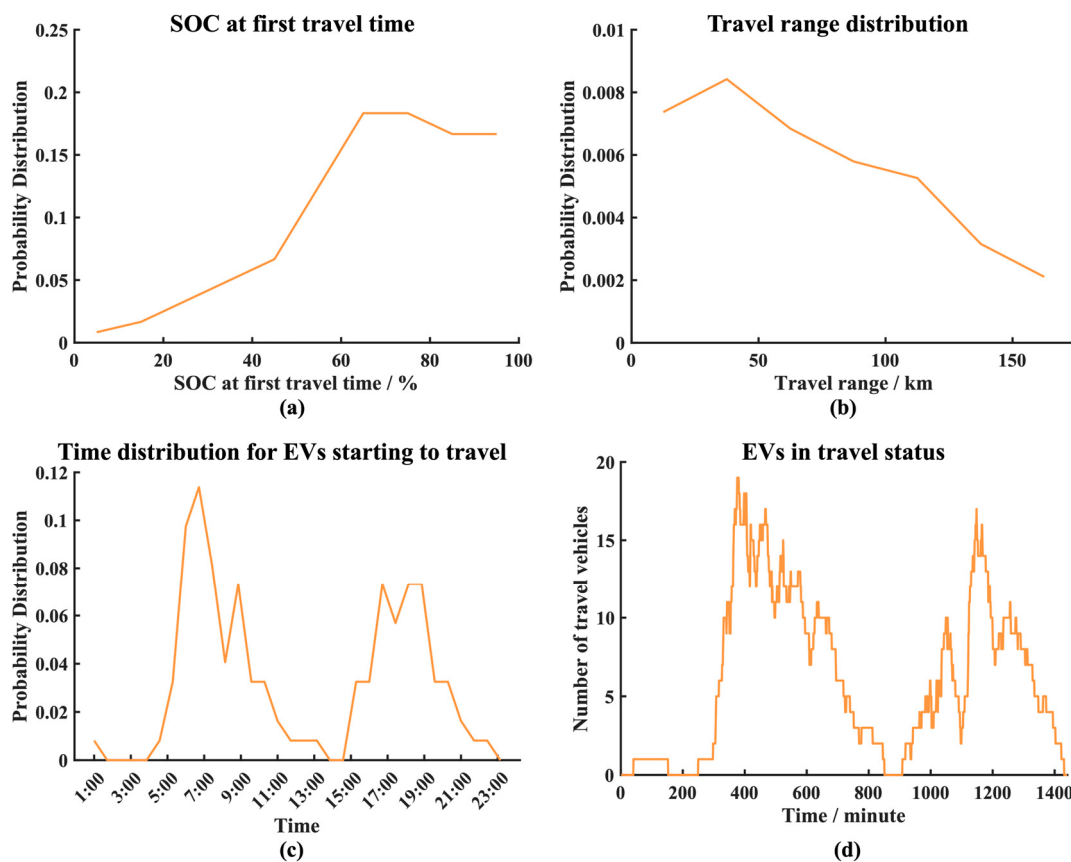


Figure 2. Travel characteristics of EVs based on Monte Carlo simulation. (a) Probability distribution of SOC at the beginning of travel and (b) travel range for EVs. (c) Time distribution of EVs starting to travel. (d) The number of EVs in travel status during a day.

These travel characteristics were used to predict the EVs' travel and charging behaviors through Monte Carlo simulations in order to estimate the charging load of EVs on a community, as presented in our previous research work [8]. The premise for applying the Monte Carlo method is to ensure that vehicle behavior is representative of real-world conditions. Therefore, based on statistical principles, we generate the travel and charging behaviors of an EV cluster, ensuring that the simulated data reflects a realistic distribution of EV usage patterns. The Monte Carlo simulation helps account for the inherent randomness and variability in EV behaviors, such as travel probability, charging time, and energy consumption. By generating a large number of random samples based on these parameters, we can simulate a broad range of possible EV charging scenarios. This approach allows us to model the uncertainties and variations in EV behavior, providing more accurate predictions for the charging load and enhancing the reliability of the results.

By incorporating the average population of 2.31 people per household in Beijing and the ownership of 100 EVs per thousand people [34,35], the analysis estimates that, by 2030, a community with 500 households would have approximately 1200 people and collectively own around 120 EVs. Using Monte Carlo simulation, the charging load of 120 EVs engaging in disorderly charging (V0G) across different time periods within a single day was obtained, as shown in Figure 3a.

China Electric Power Research Institute analyzed three years of load sample data from multiple residential communities in Beijing [36]. The analysis revealed that the baseline electricity load for residents exhibits a primary peak period from 19:00 to 23:00, a secondary peak period from 11:00 to 14:00, and a valley period from 04:00 to 07:00. According to [37], the residential electricity load curve in Beijing has remained relatively stable in recent years.

We further calculated the base electricity load for a community with 500 households in Beijing, as shown by the yellow-filled area in Figure 3b. The disorderly charging load of EVs, when superimposed on the grid's baseline load, increases the load peak from 700 kW to 790 kW. This also increased the variance of the grid load by 20.5%, exacerbating the load fluctuations, as illustrated by the red-filled area in Figure 3b. The charging load of V0G can also be regarded as the result of users engaging in charging and discharging arbitrage under constant electricity price, where the electricity price remains uniform across all time periods within a day.

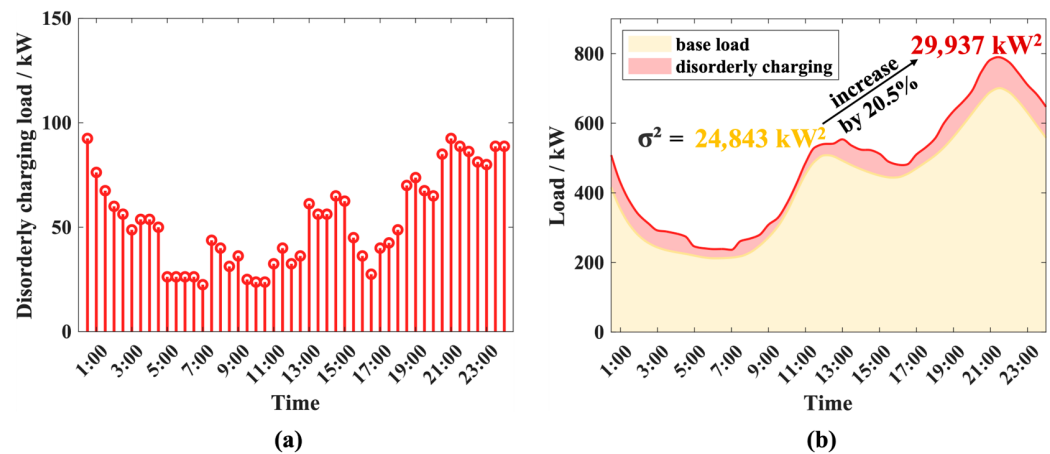


Figure 3. Monte Carlo simulation results. (a) V0G load. (b) base load + V0G load.

2.2. Battery Degradation and Energy Loss Model

The main factors affecting battery lifespan include depth of discharge (DoD) and charge/discharge rate ($C_t^{j,rate}$) [38]. To construct a battery degradation model, it is essential to comprehensively consider the losses induced by factors such as DoD and $C_t^{j,rate}$. In addition, the charging process also brings energy loss due to battery energy throughout and transformer power fluctuation. Considering all the above factors, this study develops a multi-parameter coupled model to quantify costs during the V2G charging and discharging process, as shown in Figure 4.

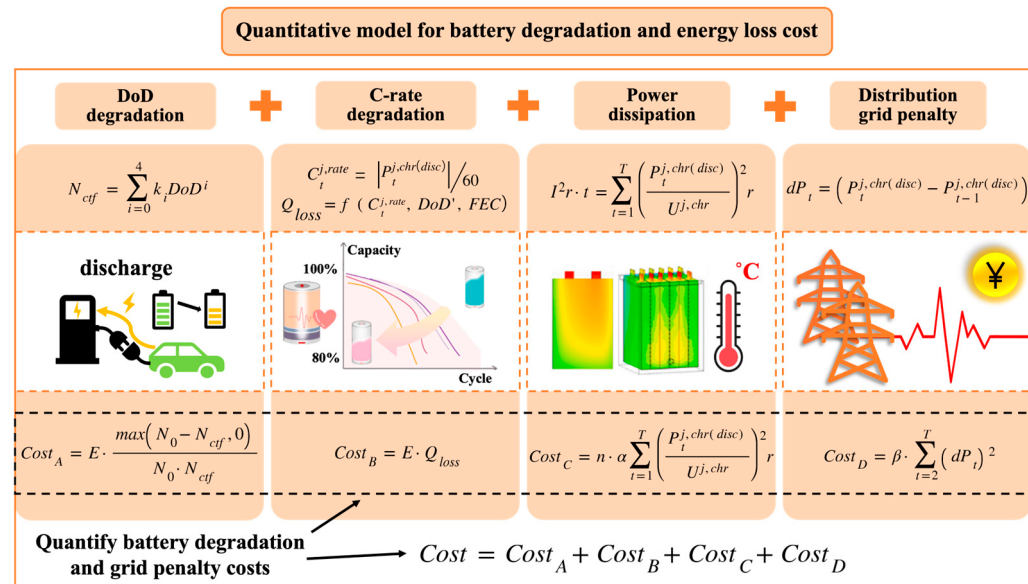


Figure 4. Overview of cost quantification models.

The battery degradation cost resulting from the daily charging and discharging behavior of EVs includes the following two components.

1. DoD: Schatz et al. [39] examined the relationship between the DoD range and battery lifespan. Based on the correlation between the battery's maximum cycle life and DoD, they proposed a single-factor DoD model using a fourth-order polynomial, as shown in Equation (1). For each complete discharge cycle of EV j when connected to the grid, its DoD is recorded. The maximum cycle life N_{ctf} of the battery under different DoD levels is calculated using Equation (1) and quantified as battery degradation cost, as shown in Equation (2).

$$N_{ctf} = 42148DoD^4 - 119140DoD^3 + 122320DoD^2 - 55583DoD + 10449 \quad (1)$$

$$Cost_A = E \cdot \frac{\max(N_0 - N_{ctf}, 0)}{N_0 \cdot N_{ctf}} \quad (2)$$

The purchase cost of the battery $E = \text{CNY } 48,000$, and the maximum cycle life at optimal battery health $N_0 = 2000$.

2. Charging/discharging rate: Naumann et al. [40] developed a semi-empirical formula model for cycle life by multiplying the effects of $C_t^{j,\text{rate}}$ and DoD, as shown in Equation (3), where FEC represents the equivalent cycle count. The battery degradation cost, considering $C_t^{j,\text{rate}}$ and DoD, is quantified as shown in Equation (4).

$$Q_{loss} = (a \cdot \sum_{t=1}^T C_t^{j,\text{rate}} + b) \cdot [c(DoD' - 0.6)^3 + d] \cdot \frac{FEC^z}{32} \quad (3)$$

$$Cost_B = E \cdot Q_{loss} \quad (4)$$

Q_{loss} represents the percentage of battery capacity degradation within a single day. The battery capacity $Cap = 60 \text{ kWh}$. The charging/discharging power of EV j at moment t is denoted as $P_t^{j,\text{chr}(\text{disc})}$. $C_t^{j,\text{rate}} = |P_t^{j,\text{chr}(\text{disc})}| / Cap$. The remaining parameter $a = 0.063$, $b = 0.0971$, $c = 4.0253$, $d = 0.00323$, $z = 0.5$, EVs average depth of discharge $DoD' = 0.8$, $FEC = 2000$.

The energy loss cost resulting from the charging and discharging process includes the following two components.

3. Energy loss cost from batteries: During the charging and discharging process of an EV, the cost associated with heat loss due to the internal resistance of the battery is calculated as the product of the energy loss and electricity price. This cost is relatively small, as shown in Equation (5).

$$Cost_C = \alpha \cdot \xi \cdot \sum_{t=1}^T \left(\frac{P_t^{j,\text{chr}(\text{disc})}}{U_t^{j,\text{chr}}} \right)^2 \cdot r \quad (5)$$

Here, the average electricity price $\alpha = 0.6 \text{ CNY/kWh}$, and $\xi = 0.0005 \text{ kWh/W}$. The average charge and discharge voltage of the battery $U_t^{j,\text{chr}} = 400 \text{ V}$, and the internal resistance of the battery pack $r = 0.1\Omega$.

4. Energy loss cost from the grid (grid penalty cost): To regulate users' charging and discharging behavior and prevent significant load fluctuations across different time periods, the grid imposes penalties on excessive variations in charging and discharging power at different times. Consequently, users are charged a related fee. For consistency with subsequent optimization objectives, these fees are combined with the

costs resulting from battery degradation and included in the user's total expenditure, as shown in Equation (6).

$$Cost_D = \beta \cdot \sum_{t=2}^T \left(P_t^{j,chr(disc)} - P_{t-1}^{j,chr(disc)} \right)^2 \quad (6)$$

Here, the penalty coefficient for power fluctuations in each period imposed by the grid β = CNY 0.02.

The user's daily expenditure related to battery degradation and energy loss are shown in Equation (7).

$$Cost = Cost_A + Cost_B + Cost_C + Cost_D \quad (7)$$

2.3. Electricity Pricing Formulation and Adjustment Strategy

The formulation of electricity pricing by the grid follows certain state flows. Figure 5 illustrates the process of electricity pricing formulation and adjustment proposed in this research.

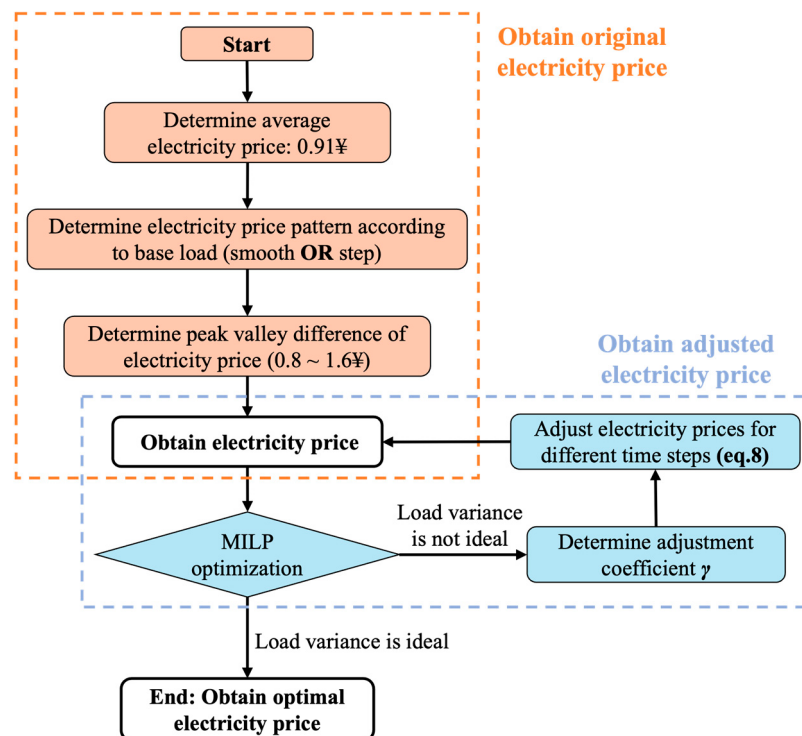


Figure 5. Process of electricity price formulation and adjustment.

2.3.1. Electricity Pricing Formulation Strategy

Electricity prices are typically positively correlated with grid load levels. When the grid load is low, electricity prices decrease, encouraging users to charge their EVs and thereby fill the grid's load valleys. Conversely, when the grid load is high, electricity prices increase, motivating users to discharge electricity back to the grid to earn revenue while simultaneously reducing peak load levels. Under this principle, as users engage in peak-valley price arbitrage, they also contribute to peak shaving and valley filling of the grid load. Figure 6 illustrates two electricity pricing models with multiple peak-valley differentials. One model features a smooth electricity price that strictly follows base load fluctuations at each moment, while the other is a step electricity price with relatively moderate changes.

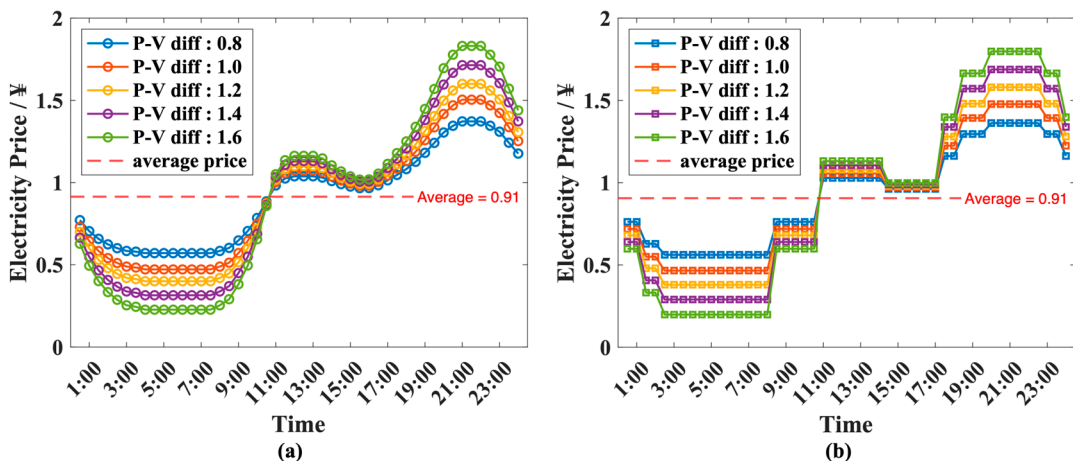


Figure 6. Multi peak–valley difference (P-V diff) electricity price. **(a)** Smooth electricity price. **(b)** Step electricity price.

2.3.2. Adjustment of Electricity Prices Based on V2G Load Fluctuations

Under different electricity prices, the grid load results derived from optimizing users' charging and discharging decisions to minimize total expenses require the grid to adjust prices. This adjustment aims to guide users toward new charging and discharging decisions, further reducing load fluctuations. At each moment, when the grid load is below the daily average, the electricity price at that moment is reduced to encourage users to charge their devices. Conversely, when the grid load exceeds the daily average, the electricity price at that moment is increased to encourage users to discharge electricity back to the grid.

The electricity price adjustment rule is shown in Equation (8). EPc_t^{i-1} denotes the electricity price at moment t before round i of adjustments. The original, unadjusted electricity price is denoted as EPc_t^0 , EPc_t^i denotes the electricity price at moment t after round i of adjustments, and $P_t^{chr,i-1}$ represents the total charging and discharging power of EVs at moment t before round i of adjustments. L_t^{i-1} denotes the base load at time t before round i of adjustments. avg^{i-1} denotes the average grid load before round i of adjustments, and γ_i represents the coefficient for round i of adjustments.

$$EPc_t^i = EPc_t^{i-1} + \gamma_i \cdot \left(\left(P_t^{chr,i-1} + L_t^{i-1} \right) - avg^{i-1} \right) \quad (8)$$

Whether electricity prices need to be adjusted depends on the fluctuations in grid load, which are measured using relative fluctuation (R_f). The calculation of relative fluctuation is shown in Equation (9), where σ represents the standard deviation of the grid load under a specific scenario, and $Range_{V0G}$ denotes the grid load range under the V0G scenario (users participating in arbitrage under constant electricity pricing).

$$R_f = \frac{\sigma}{Range_{V0G}} \times 100\% \quad (9)$$

In Figure 3b, the grid load variance under the V0G scenario is 29,937 kW², with a standard deviation of 173 kW and a relative fluctuation of 31.81%. The economic load rate of distribution transformers in residential communities is typically 65% [41]. In the scenario studied in this paper, where 30% of EVs participate in V2G, we set 10% of the economic load rate as the ideal load fluctuation limit. Therefore, a relative fluctuation of the grid load below 6.50% is considered ideal, and no further electricity price adjustments are required.

In order to stabilize the grid load with as few adjustment rounds as possible, the selection of electricity price adjustment coefficient γ_i in Equation (8) is related to the load relative fluctuation R_f in Equation (9). In round i of adjustments, when relative fluctuation

before adjustment is large ($R_f > 10\%$), the coefficient is selected as 0.001. When the relative fluctuation is small ($6.5\% < R_f \leq 10\%$), due to the limited difference between grid load and its average value, the coefficient can be expanded to 0.00175, as shown in Equation (10).

$$\begin{cases} \gamma_i = 0.001 & R_f > 10\% \\ \gamma_i = 0.00175 & 6.5\% < R_f \leq 10\% \\ \gamma_i = 0 & R_f \leq 6.5\% \end{cases} \quad (10)$$

2.4. Mixed-Integer Linear Optimization (MILP) Aimed at Minimizing Users' Total Expenditure

To formulate reasonable electricity prices, it is necessary to obtain information about the grid load. Therefore, optimizing the charging and discharging decisions that minimize users' total expenditure is essential. This study adopts mixed-integer linear programming (MILP), using YALMIP functions to set nonlinear boundary constraints and employing the Gurobi solver to perform the optimization.

Establishing the power and energy boundaries of a single vehicle is necessary for optimization. The state of the EV j at moment t needs to satisfy the following constraints. Equations (11) and (12) define the power and energy constraints for EV j . Equation (13) expresses that EV can only choose one state of charging, discharging and not accepting dispatch at any scheduling time. Equation (14) specifies that EV j scheduling is restricted to the parking phase. Equation (15) represents the energy state of EV j at moment t . Equation (16) indicates that the total daily charging amount for a user must meet travel demands, where h represents the electricity consumption per 100 km for the EV ($h = 16 \text{ kWh}/100 \text{ km}$), and Range_{travel}^j denotes the travel distance of EV j .

$$P_t^{j,LB} \leq P_t^{j,chr(disc)} \leq P_t^{j,UB} \quad (11)$$

$$E_t^{j,LB} \leq E_t^j \leq E_t^{j,UB} \quad (12)$$

$$S_t^{j,chr} + S_t^{j,disc} \leq 1 \quad (13)$$

$$S_t^{j,chr} + S_t^{j,disc} = 0 \quad (t \notin T) \quad (14)$$

$$E_t^j = E_0^j + \sum_{\tau=1}^t (P_{\tau}^{j,chr} + P_{\tau}^{j,disc}) \cdot \Delta t \quad (15)$$

$$\sum_{t=1}^T (P_t^{j,chr} + P_t^{j,disc}) \cdot \Delta t \geq h \cdot \text{Range}_{travel}^j \quad (16)$$

For an EV cluster consisting of N vehicles, the charging/discharging state after EVs connect to the grid is determined by the 0–1 variables $S_t^{j,chr}$ and $S_t^{j,disc}$ for EV j at moment t . This leads to the relationship between the total charging/discharging power P_t^{chr} at moment t and the charging/discharging power $P_t^{j,chr}, P_t^{j,disc}$ of EV j at moment t :

$$P_t^{chr} = \sum_{j=1}^N (S_t^{j,chr} P_t^{j,chr} + S_t^{j,disc} P_t^{j,disc}) \quad (17)$$

The grid must ensure that the load at the initial moment of the day ($t = 1$) equals the load at the final moment of the day ($t = T$), maintaining the generality of regional load across different days, as shown in Equation (18).

$$P_1^{chr} + L_1 = P_T^{chr} + L_T \quad (18)$$

where L_1 and L_T represent the base load of the grid at the initial and final moments of the day.

The electricity cost for EV j is denoted as $ePrice^j$, as shown in Equation (19). The total expenditure of users includes electricity cost, battery degradation cost, and energy loss cost. The optimization objective of minimizing the total expenditure can be expressed by Equation (20).

$$ePrice^j = \frac{24}{T} \cdot \sum_{t=1}^T \left(S_t^{j,chr} \cdot P_t^{j,chr} \cdot EPc_t - S_t^{j,disc} \cdot P_t^{j,disc} \cdot EPc_t \right) \quad (19)$$

$$\text{Objective} = \min \left(\sum_{j=1}^N (ePrice^j + Cost^j) \right) \quad (20)$$

The battery degradation cost and energy loss cost for EV j are denoted as $Cost^j$.

3. Case Study and Results Analysis

3.1. Optimal Electricity Price and Peak Shaving and Valley Filling in Load Management

3.1.1. Selection of the Original Electricity Price

Considering smooth and stepped TOU electricity pricing structures with various fluctuation range, the grid load profiles are derived after EV users minimizes their total expenditures according to Equation (20). This analysis incorporates various battery degradation and energy loss models, with the resulting load variance of the grid illustrated in Figure 7.

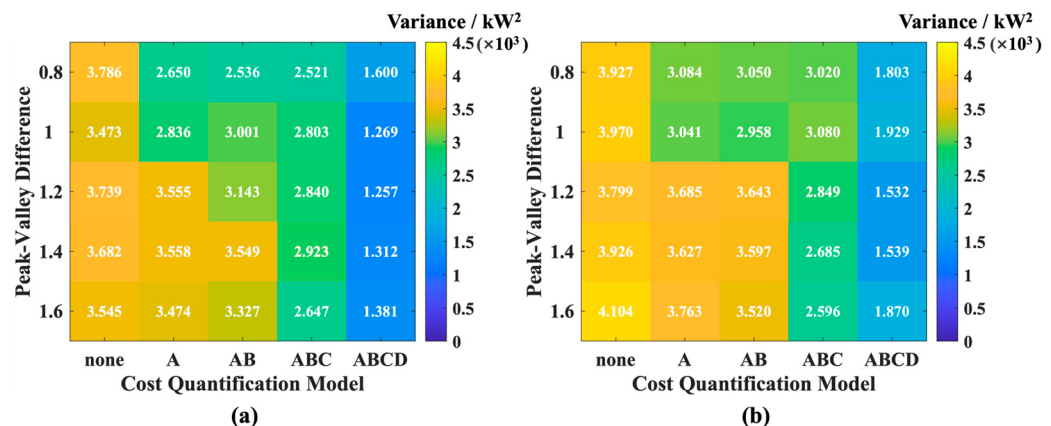


Figure 7. Load variance result after optimizing under various peak–valley price difference and degradation model. (a) Smooth TOU electricity price as shown in Figure 6a. (b) Step TOU electricity price as shown in Figure 6b.

In Figure 7, “none” represents the scenario without considering battery degradation or energy loss cost. “A” accounts for battery degrading only influenced by *DoD*, “AB” further includes battery degrading influenced by charge/discharge rate, “ABC” further added energy loss cost in battery side, and “ABCD” considers all cost factors, as in Equation (7).

The grid’s objective is to minimize load fluctuations as much as possible.

Within the multi-parameter coupling model that quantifies V2G costs (“ABCD” in Figure 7), this study evaluates both smooth and stepped electricity price strategies. Based on smooth electricity price with peak–valley differentials of CNY 1.0, CNY 1.2, and CNY 1.4, the grid load variance deriving from user’s optimal decision are obtained. Similarly, the corresponding stepped electricity price strategies with the same peak–valley differentials are also analyzed. Under a scenario where 30% of EVs participate in V2G, Table 1 presents the net revenue from grid load, revenue from selling electricity to EVs, expenditure for

purchasing electricity from EVs, revenue from the baseline load, and revenue from selling electricity to the 70% of EVs that do not participate in V2G. The net revenue of the grid is the same as the sum of the other four cost items in Table 1, where (–) indicates payments made by the grid to users. V2G operation mode between grid and user is shown in Figure 8.

Table 1. Electricity revenue and expenditure of distribution grid under different electricity prices.

Pricing Pattern	Peak–Valley Difference	Net Revenue Obtained from Grid Load	30% V2G Revenue from Selling Electricity to EVs	30% V2G Expenditure on Purchasing Electricity from EVs	Base Load Electricity Revenue	70% V0G Revenue from Selling Electricity to EVs
Smooth	CNY 1.0	CNY 10,036	CNY 722	(–)CNY 2079	CNY 10,623	CNY 770
	CNY 1.2	CNY 10,033	CNY 627	(–)CNY 2209	CNY 10,839	CNY 776
	CNY 1.4	CNY 10,025	CNY 514	(–)CNY 2324	CNY 11,094	CNY 741
Segmented	CNY 1.0	CNY 9933	CNY 652	(–)CNY 1997	CNY 10,559	CNY 719
	CNY 1.2	CNY 9927	CNY 578	(–)CNY 2213	CNY 10,810	CNY 752
	CNY 1.4	CNY 9905	CNY 467	(–)CNY 2382	CNY 11,072	CNY 748

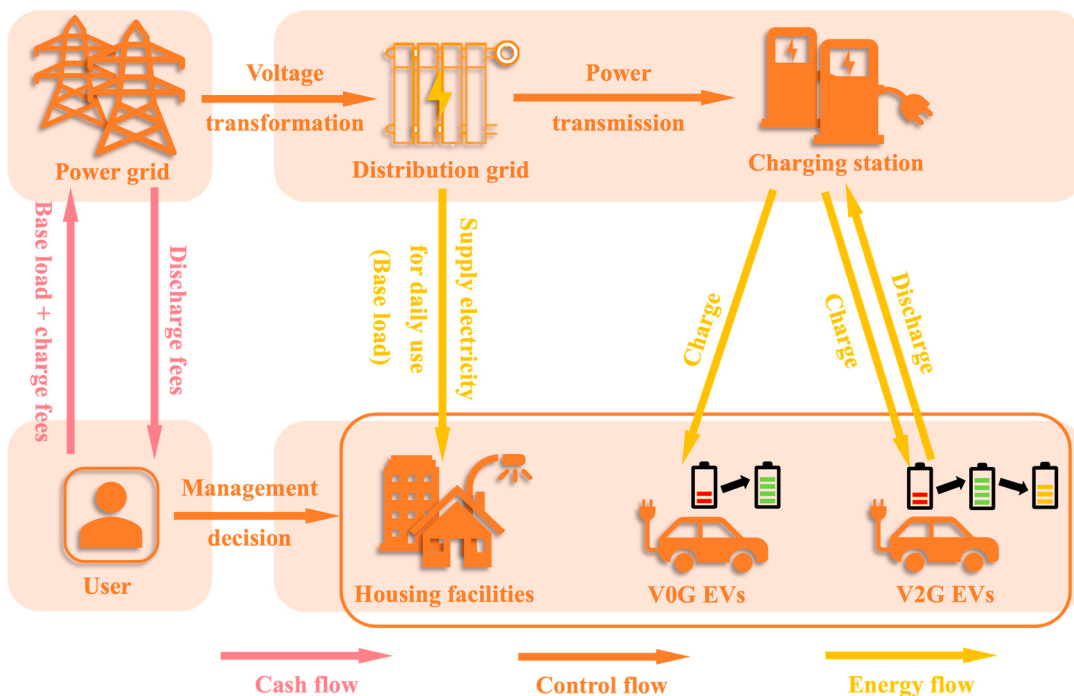


Figure 8. V2G cash flow between power grid and user.

As shown in Table 1, under 30% V2G participation, the grid's net revenue is higher with a smooth electricity price compared to a stepped electricity price, though no clear maximum value is observed. Considering that the grid load variance is lower under a smooth price than a stepped price, the price scheme with the minimum load variance ($1.257 \times 10^3 \text{ kW}^2$) and relatively high grid revenue—a smooth electricity price with a peak–valley differential of CNY 1.2—is selected as the original electricity price. This price will be adjusted in subsequent analysis.

3.1.2. Adjustment of Electricity Price to Achieve Ideal Peak–Valley Load Difference

Under a smooth electricity price with a peak–valley differential of CNY 1.2, and with the objective of minimizing users' total expenditure, the grid load without considering V2G cost is shown in Figure 9a. The grid load that considers the multi-parameter coupling model

for V2G cost is shown in Figure 9b. To achieve this result, two rounds of price adjustments are carried out with adjustment coefficients $\gamma_1 = 0.001$, $\gamma_2 = 0.00175$. The electricity prices before and after the adjustments are shown in Figure 9c, with the grid load illustrated in Figure 9d. At this point, the effect of users participating in V2G on the grid load has reached an ideal state. However, a load peak still occurs during 20:00–24:00, as all EVs connected to the grid in this period are discharging. Despite this, the original peak of the base load cannot be entirely fully shaved. Figure 9e presents the total charging/discharging power extraction under 30% V2G and 100% V0G in this scenario. Figure 9f,g illustrate the changes in energy and power for EVs participating in V2G throughout the day. EVs numbered 1–11 represent those with two trips during the day, EVs numbered 12–19 represent those with one trip, and EVs numbered 20–36 represent those that do not travel throughout the day.

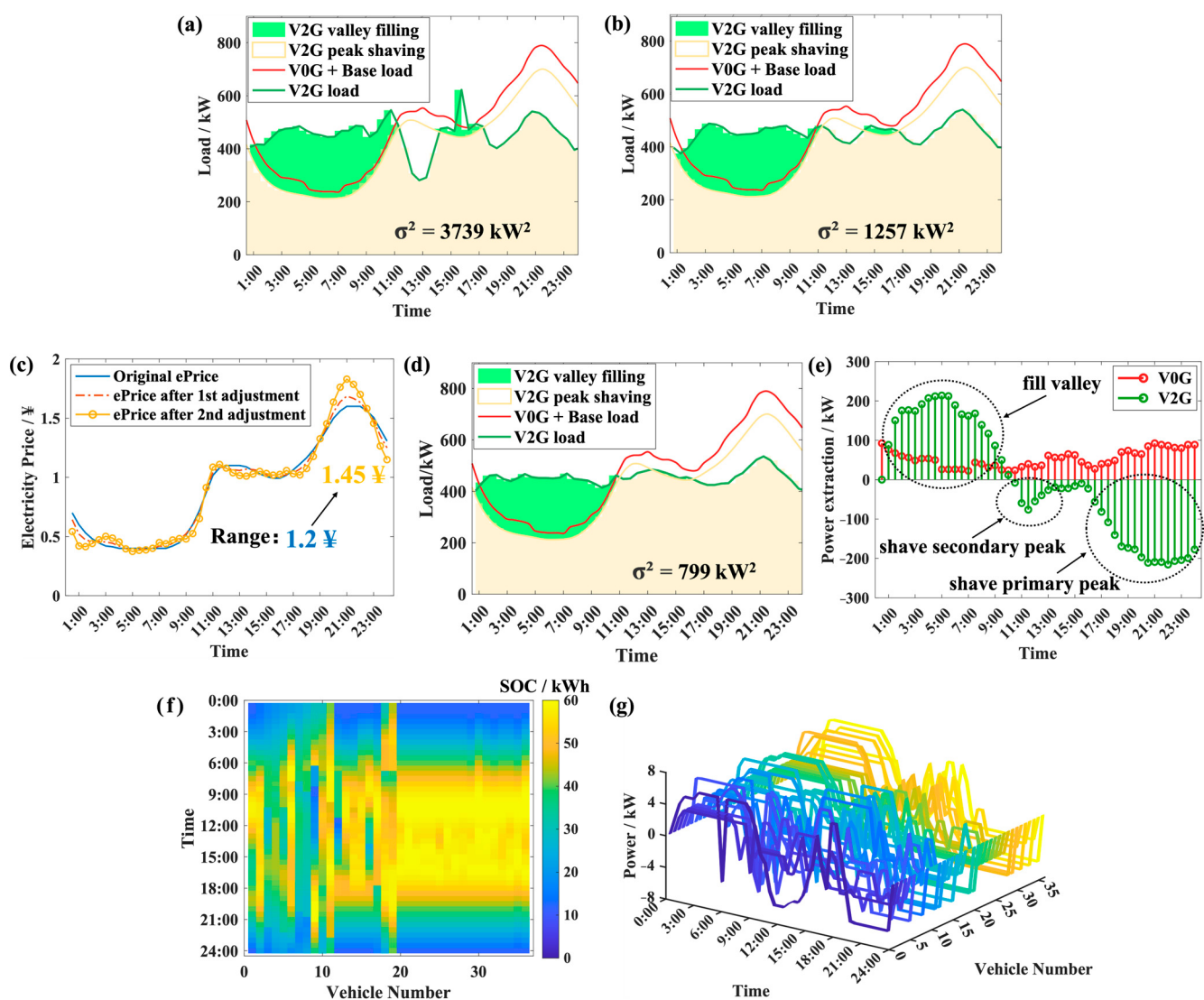


Figure 9. Optimization results based on smooth electricity price with peak valley difference of CNY 1.2. (a) Optimized load without considering any battery degradation or energy loss and (b) optimized load considering complex cost models. (c) The TOU electricity price during the two rounds of electricity price adjustment and (d) grid load result considering complex V2G cost models based on electricity prices after the 2nd adjustment and its (e) total power extraction from EVs and the corresponding (f) SOC change and (g) power curve of the EVs participating in V2G.

Considering the V2G operation costs, the load variance decreases from 3739 kW^2 to 1257 kW^2 , and the standard deviation decreases from 61.2 kW to 35.5 kW . According to Equation (9), the relative fluctuation decreases from 11.24% to 6.52%. After two rounds of electricity price adjustments, the load variance decreases from 1257 kW^2 to 799 kW^2 , while the relative fluctuation reduces from 6.52% to 5.19%. During the two rounds of electricity price adjustments, the peak-to-valley price differential increased from CNY 1.2 to CNY 1.45, but the average electricity price remained unchanged. Under a 30% V2G participation scenario, the grid's net revenue from grid load, consisting of revenue from selling electricity to EVs, expenditure on purchasing electricity from EVs, base load revenue, and revenue from selling electricity to the EVs not participating in V2G, is shown in Figure 10. Before and after the electricity price adjustment, the grid's revenues and expenditures basically remained unchanged.

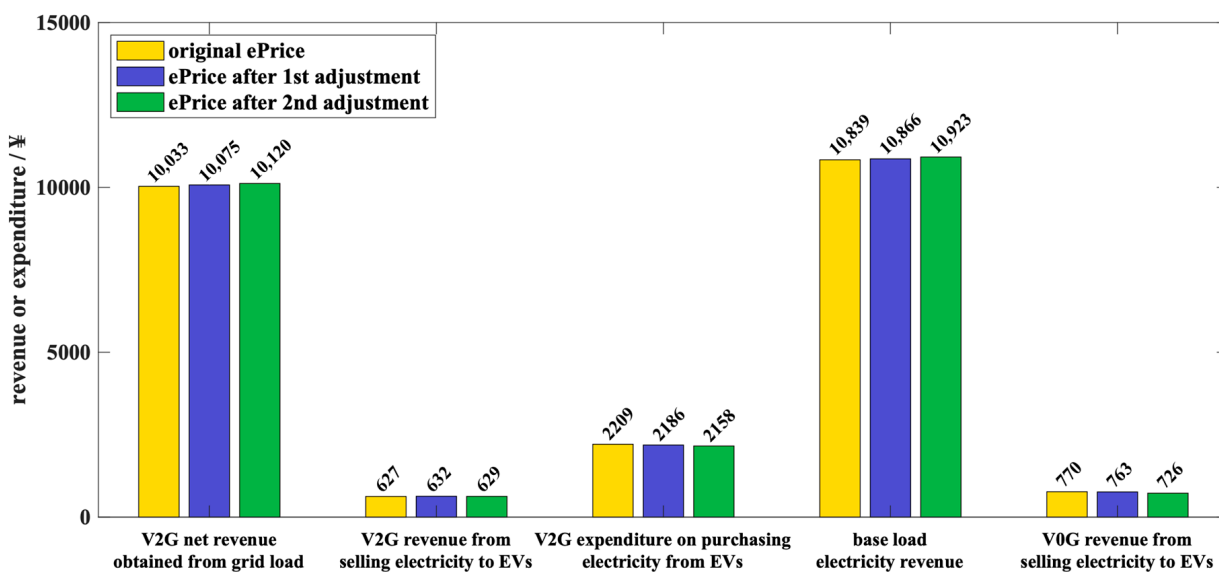


Figure 10. Electricity revenue and expenditure under prices before and after adjustment.

3.2. Power and Energy Analysis of EVs

After obtaining the optimization results under the adjusted electricity prices, the charging and discharging behaviors of typical EVs are selected to analyze the effect of different categories: no travel, one travel per day, and two travels per day. The power and energy changes of typical EVs with different travel frequencies are shown in Figure 11.

The yellow bars in Figure 11 represent the charging power of EVs under V0G. In the V0G scenario, EVs that do not travel throughout the day have no charging demand and do not increase the grid load. The disorderly charging load of EVs with one trip occurs during periods when the grid experiences secondary peak loads (11:00 to 14:00). For EVs with two trips, their disorderly charging load mainly occurs during periods when the grid experiences primary peak loads (19:00 to 23:00).

In V2G scenario, EVs can connect to the grid during non-travel periods and make charging/discharging decisions based on user preferences to achieve arbitrage and minimal cost. Since EVs that do not travel throughout the day can perform charging/discharging scheduling at any time without a total charging demand, they have the most significant effect on peak shaving and valley filling of the grid load.

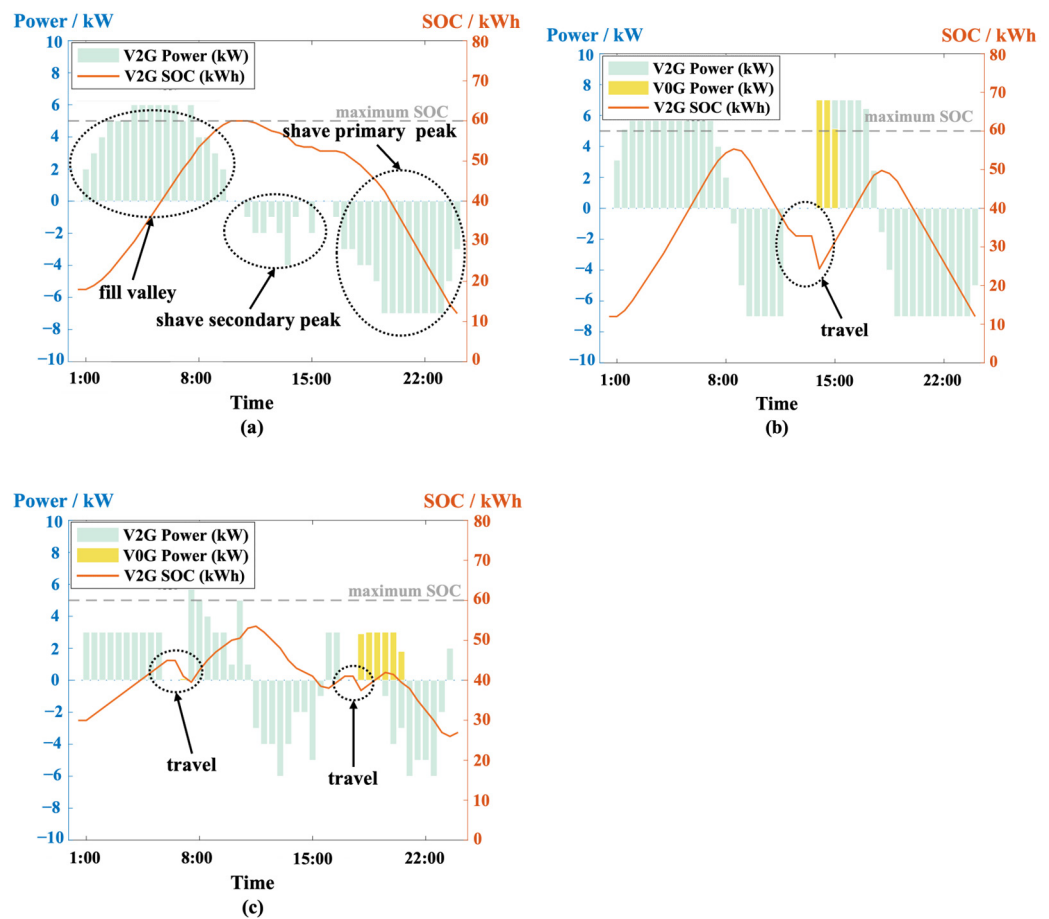


Figure 11. The V0G and V2G power variation and V2G energy curve of vehicles that travel (a) 0 times, (b) 1 time, and (c) 2 times a day.

3.3. Analysis of V2G Decision and Profits of EVs

3.3.1. Charging/Discharging Requirement and Electricity Price Adjustment

Based on the optimization decision under the adjusted electricity prices, the charging behaviors of EVs under V2G was analyzed, and an equivalent charging demand is presented. Figure 12 illustrates the equivalent charging demand for EVs with different travel frequencies. The daily time periods for EVs are divided into equivalent charging periods, travel periods, and arbitrage periods. For each period during which an EV is connected to the grid:

1. If the EV's charging energy exceeds its discharging energy, the EV is considered to be undergoing actual charging during this period, which is classified as an equivalent charging period.
2. If the EV's charging energy is less than or equal to its discharging energy, the EV is considered not to be undergoing actual charging during this period, which is classified as an arbitrage period.
3. The energy consumption of each EV trip is evenly distributed into the equivalent charging periods to calculate the equivalent charging load.

The accumulated equivalent charging demand of EVs participating in V2G is represented by the blue spikes in Figure 13. Compared to the V0G scenario, the charging load after 11:00 shows a reduction, indicating that arbitrage behavior induces a shift in the actual charging periods of EVs. EVs tend to charge before 11:00 under V2G.

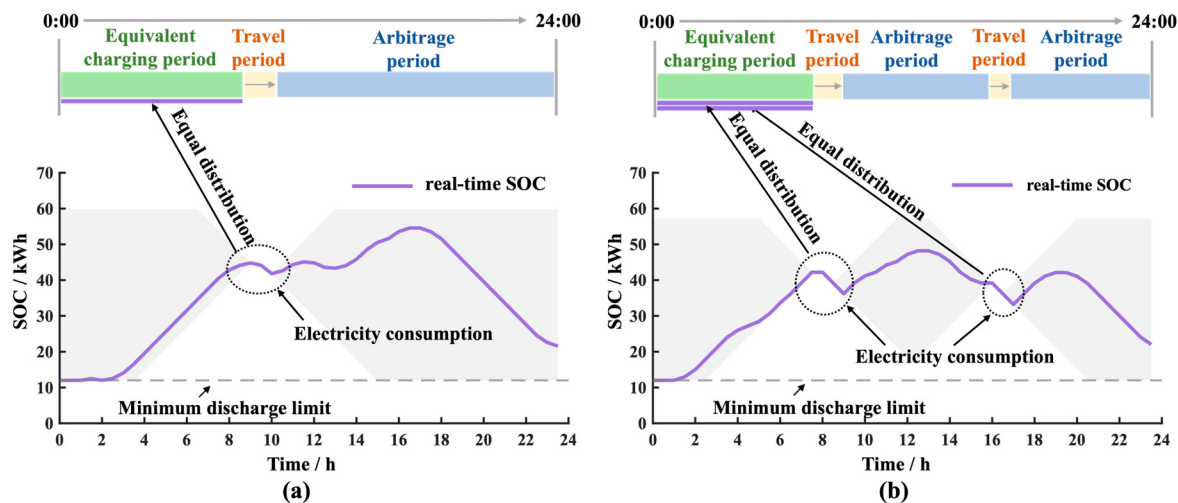


Figure 12. Principle of classifying equivalent charging periods, travel periods, and arbitrage periods for EVs with (a) 1 travel period and (b) 2 travel periods per day.

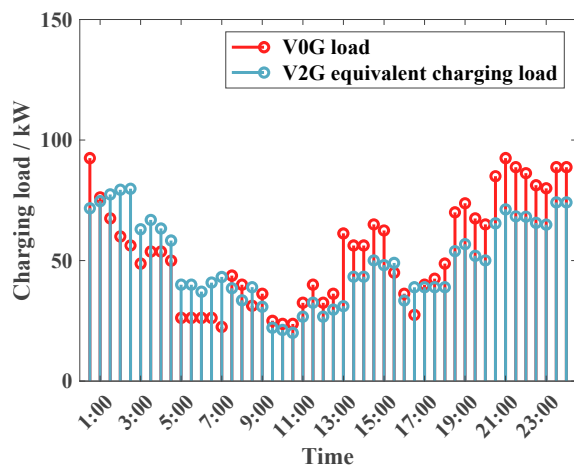


Figure 13. V2G equivalent charging load and V0G load.

Since each round of electricity price adjustments is based on the previous day's grid load results, there exists a lag in load optimization. Therefore, it is necessary to analyze real-time characteristics related to EVs' electricity consumption and travel patterns, enabling the grid to achieve real-time electricity price adjustments within the initial pricing process and eliminate the lag in load optimization. Extracting the travel and electricity consumption characteristics of EVs, and analyzing their relationship with the total adjustments made in the two rounds of electricity price changes, aims to identify underlying patterns for guiding future electricity price adjustment strategies.

Using the feature extraction method based on Lasso regression [42], it is found that the total amount of electricity price adjustments is strongly correlated with the increasing or decreasing trend of the equivalent charging load of the EV cluster. By analyzing the positive and negative signs of their derivatives at different time periods, it is found that they exhibit the same positive or negative trend (including cases where one of them equals 0) in 66% of the periods throughout the day, as shown by the green shading in Figure 14. During periods of increasing equivalent charging load, the grid can raise electricity prices. Correspondingly, during periods of decreasing equivalent charging load, the grid can lower electricity prices.

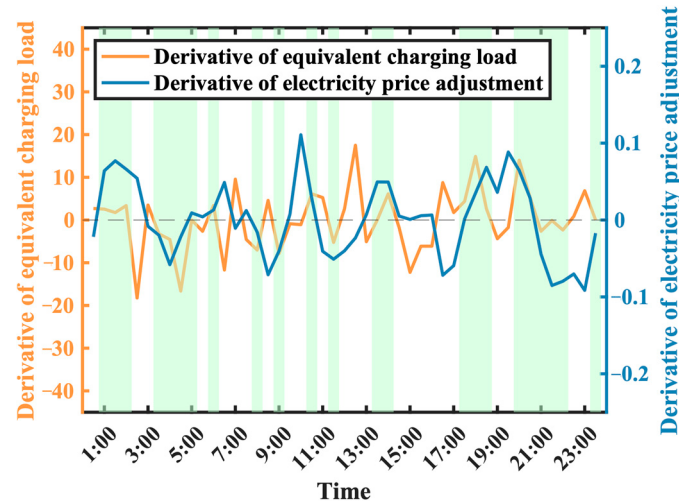


Figure 14. Correlation between derivative of equivalent charging load and electricity price adjustment.

3.3.2. Revenue and Expenditure

For all EVs participating in V2G arbitrage (a total of 36 vehicles), the distributions of energy throughput, battery degradation and energy loss cost, electricity price cost/arbitrage revenue, and total cost/net revenue under the V2G scenario and the corresponding V0G scenario are shown in Figure 15a, 15b, 15c and 15d, respectively.

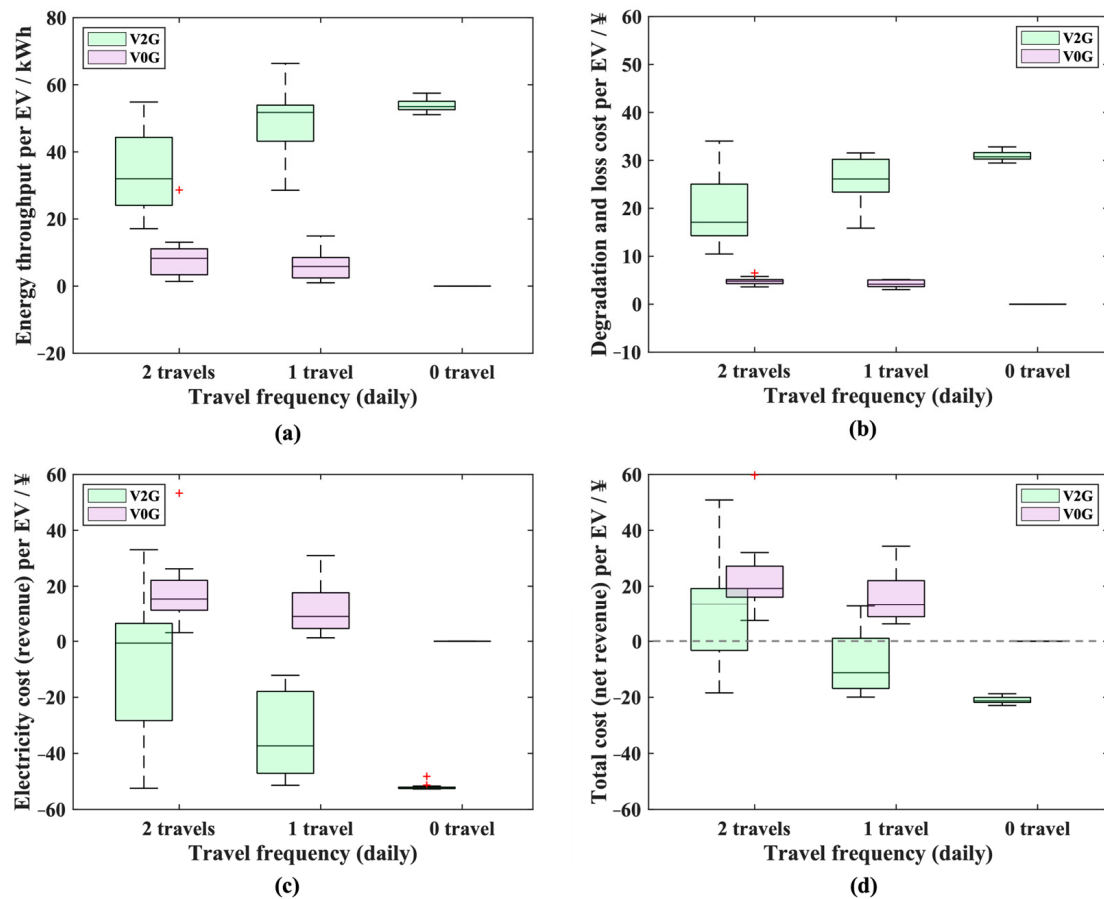


Figure 15. (a) Energy throughput, (b) degradation and energy loss cost, (c) arbitrage revenue from TOU electricity price, and (d) net profits of EVs with different travel frequency.

In the V0G scenario, EVs with two travel periods per day and those with one travel period per day have similar energy throughput, battery degradation and energy loss cost, TOU electricity price revenue, and net profit. EVs that do not travel throughout the day exhibit no charging demand, resulting in no energy throughput or associated cost.

In the V2G scenario, as the travel frequency decreases, the time EVs can connect to the grid for arbitrage increases, leading to a gradual rise in energy throughput, which is significantly higher than that in V0G scenario. Consequently, this intensifies the battery degradation and energy loss cost, which are significantly higher than those in the V0G scenario, as shown in Figure 15a,b. Meanwhile, as the travel frequency decreases, electricity price cost and total cost decrease (arbitrage revenue and net revenue increase). Under the condition of meeting travel demands, 54.5% of EVs with two travel periods, as well as all EVs with one travel period and no travel, can achieve net revenue through arbitrage (indicated by negative electricity price costs), as shown in Figure 15c. Considering battery degradation and energy loss cost, 27.3% of EVs with two travel periods, 75% of EVs with one travel period, and all EVs with no travel can still obtain profits, as shown in Figure 15d. The energy throughput distribution of EVs with no travel throughout the day leads to concentrated distributions of battery degradation and energy loss costs, arbitrage revenue, and net revenue. This suggests that, in the context of this study, the charging/discharging decisions of non-traveling EVs are uniform.

The total cost of all EVs participating in V2G (36 vehicles) under different cost quantification models is shown in Figure 16. In order to quantify the cost of peak–valley arbitrage for V2G, we can distribute the cost of battery degradation and energy loss, as in Equation (7), into the discharging energy of EVs for V2G, as shown in Equation (21). The life degradation coefficient of EVs is represented by μ .

$$\text{Cost} = \mu \cdot \sum_{t=1}^T E_{disc}^j \quad (21)$$

Based on Equation (21), the calculation yields $\mu = 0.608$ CNY/kWh, which is approximately the same as the cost of degradation during the charging/discharging process of EV batteries. The average life degradation coefficient of the current EV battery is approximately 0.6 CNY/kWh (calculated based on a battery price of 600 CNY/kWh, with a cycle life of 1000 cycles). As the life of EV batteries extends in the future, the average life degradation coefficient will decrease, resulting in greater profits from V2G arbitrage.

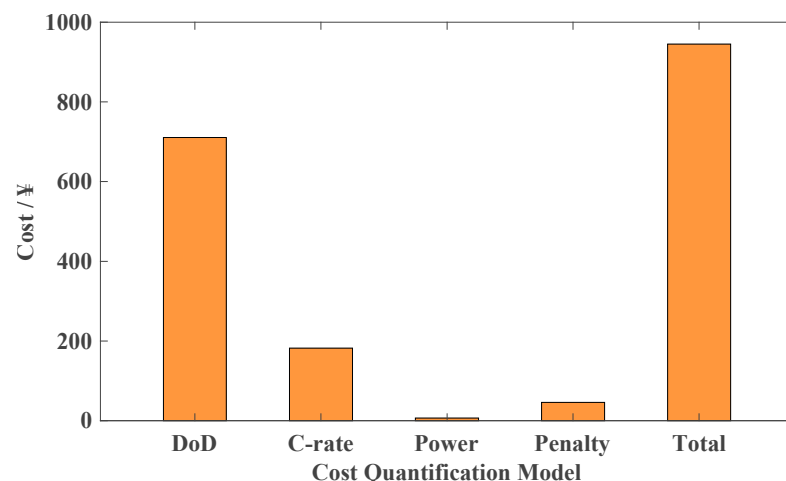


Figure 16. Total cost of EVs participating in V2G under different cost quantification models.

Table 2 presents the total annual average data of battery lifespan loss, energy throughput and charge–discharge cycle for single EV under different travel frequencies. Under the same travel frequency, the energy throughput and battery lifespan loss of EVs participating in V2G arbitrage are significantly higher than those of V0G (by an order of magnitude or more). As V2G technology becomes more widespread, this result will have a significant impact on the energy storage system and the battery industry.

Table 2. Total annual average data of battery lifespan loss, energy throughput and charge–discharge cycle.

	Total Annual Data per EV	2 Travel Periods per Day	1 Travel Period per Day	0 Travel Periods per Day
V2G	Battery lifespan loss per year	2.9%	3.9%	4.7%
	Energy throughput per year	12,297 kWh	17,912 kWh	19,685 kWh
	Charge–discharge cycle per year	102.4	149.2	164.1
V0G	Battery lifespan loss per year	0.7%	0.6%	0
	Energy throughput per year	3256 kWh	2261 kWh	0
	Charge–discharge cycle per year	27.1	18.9	0

In 2025, China is expected to have 31.4 million EVs [43]. Based on the travel probabilities of the EV cluster in this paper, assuming that 30% of the EVs participate in V2G and operate in energy arbitrage during all non-travel periods, it is estimated that an additional 102,200 GWh of energy throughput will be generated nationwide in 2025. This is equivalent to 0.06% of China's annual electricity consumption (approximately 170,000,000 GWh). Concurrently, this effectively corresponds to the saving of the installation of an energy storage facility with a capacity of 350 GWh, which undergoes one charge–discharge cycle per day within an SOC range of 80%.

Each EV participating in V2G experiences an average annual battery lifespan loss of approximately 4%. Under a healthy battery state where SOH > 80%, it can engage in V2G for at least 5 years. The average net revenue that each EV can generate over 5 years is CNY 15,330, considering both battery degradation and energy loss costs.

4. Discussion

4.1. EV Battery Lifespan

With the improvement of EV battery lifespan, the cost caused by battery degradation during charging/discharging processes will decrease. This section analyzes the impact of cost reductions caused by DoD and C-rate in the battery degradation model on grid load as well as users' V2G arbitrage revenues and expenditures. Based on the electricity price result after two rounds of adjustments, the coefficient of degradation costs caused by DoD and C-rate reduced by 50%, and the optimized grid load resulted from the user's maximal profit decision, as shown in Figure 17a. The total costs of battery degradation and energy loss for the EV cluster participating in V2G are illustrated in Figure 17b.

With the cost reduction caused by battery degradation, the variance of grid load rose from 799 kW^2 to 1187 kW^2 , and the relative fluctuation increased from 5.19% to 6.33%. However, the fluctuation remains minimal and is still within the ideal range. This indicates that the current electricity price remains applicable even as the battery lifespan improves. The total cost of battery degradation and energy loss for the vehicle cluster decreases by 49.2%. According to Equation (21), the average life degradation coefficient decreases from CNY 0.608 to CNY 0.345.

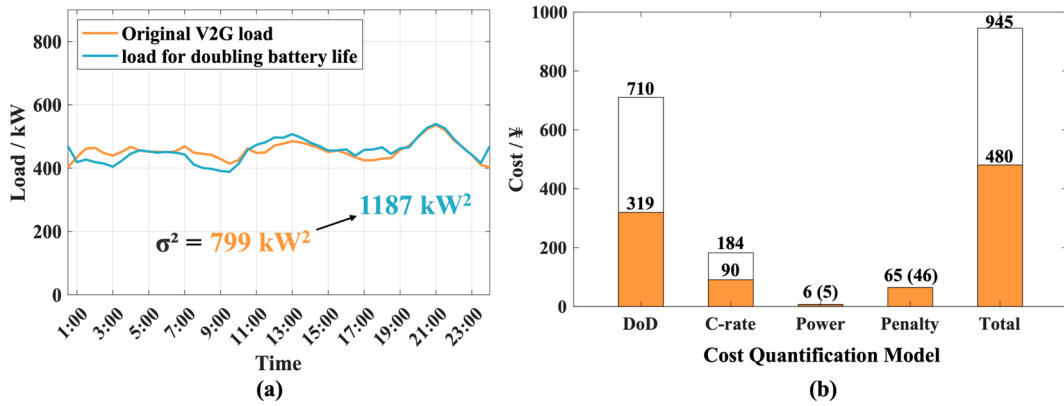


Figure 17. (a) Grid load before and after the degradation coefficient reduction under 30% V2G, and (b) cost composition of EV cluster before (white bar) and after (orange bar) battery lifespan extension.

4.2. V2G Participation Ratios

With the advancement of grid intelligence and the promotion of relevant policies, the proportion of users participating in V2G for arbitrage is expected to increase. This section analyzes the impact of user participation rates in V2G on the grid load and electricity price adjustments.

Under different V2G participation ratios, the impact of smooth electricity prices with varying peak–valley differences on the grid load is shown in Figure 18.

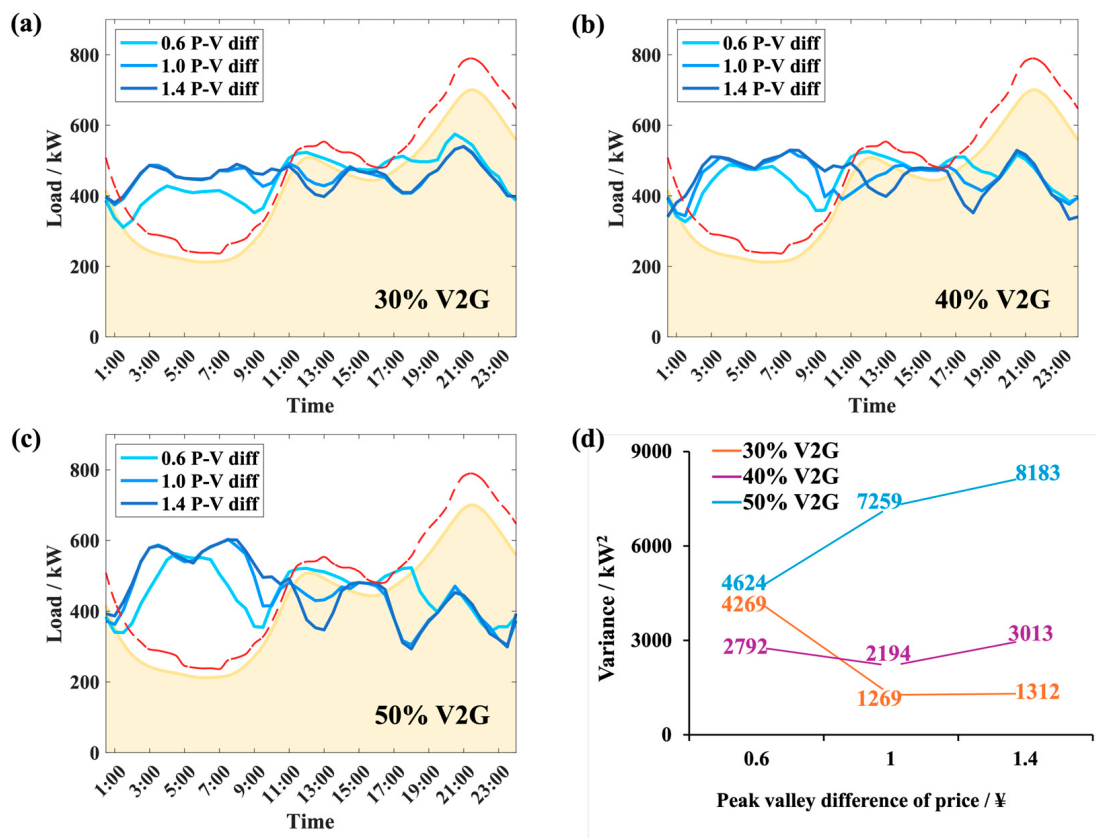


Figure 18. Grid load under the maximal net profits of EVs, in the scenario of (a) 30%, (b) 40%, and (c) 50% of EVs participating in V2G under different peak valley differences (P-V diff) in electricity prices and (d) load variance under different V2G participation rates and peak valley differences in electricity prices.

As the V2G participation ratio increases, the fluctuation in grid load tends to rise at high peak–valley difference in electricity price, requiring a reduction in the peak–valley difference of electricity prices to avoid peaks in charging loads. The results indicate that when the V2G participation ratio increases (up to 50%), reducing the peak–valley difference in electricity prices (to CNY 0.6) can partially mitigate the increase in load fluctuations, as shown by the blue line in Figure 18d. However, the effect is not ideal. To further reduce load fluctuations, it is necessary to adjust prices according to Equations (8) and (10).

Under 50% V2G, the original electricity price with the smallest load variance (smooth electricity price with an initial peak–valley difference of CNY 0.6) is adjusted through two rounds with $\gamma_1 = 0.001$, $\gamma_2 = 0.00175$, as shown in Figure 19a. The peak–valley difference of the optimal electricity price is CNY 0.61. The load situation after two rounds of electricity price adjustments is shown in Figure 19b. At this point, the load variance decreases from 4624 kW^2 to 1185 kW^2 , the standard deviation decreases from 68 kW to 34.4 kW , and the relative fluctuation drops from 12.50% to 6.32%, achieving an ideal state.

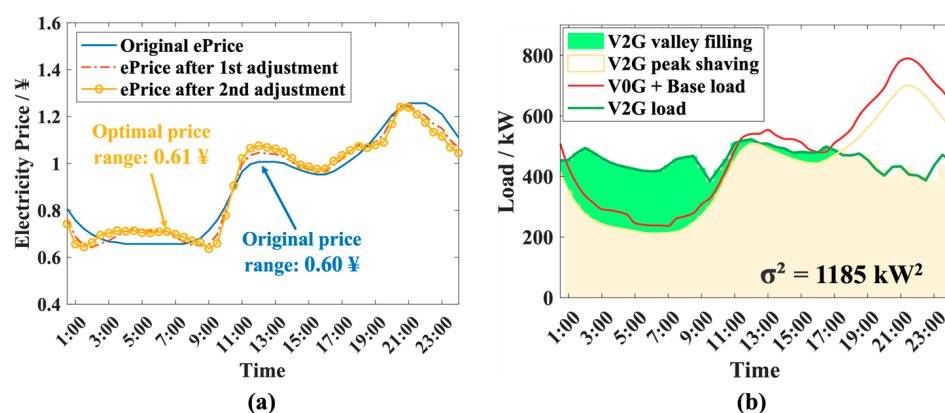


Figure 19. The (a) electricity price adjustment and (b) optimized load under 50% V2G.

The net revenue of the grid before and after the electricity price adjustments is shown in Figure 20. Compared to 30% V2G, the grid's net revenue under 50% V2G shows no significant change, indicating that this electricity price adjustment strategy can still ensure stable grid revenue as the V2G participation ratio increases.

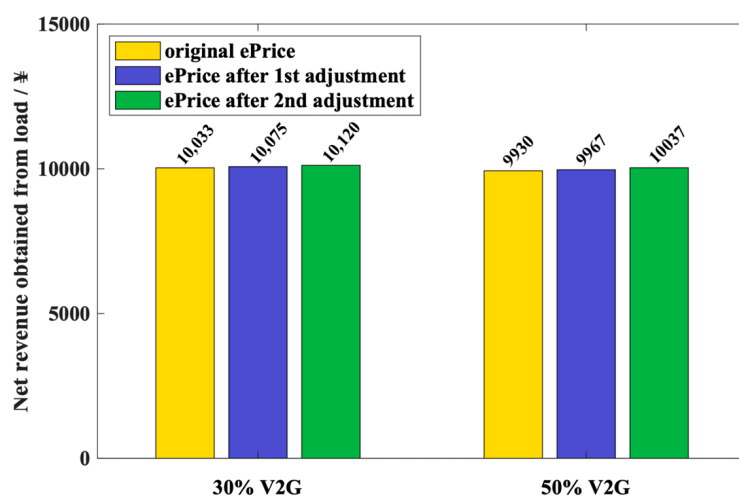


Figure 20. Net revenue of the grid before and after electricity price adjustment under different V2G participation rates.

5. Conclusions

Based on the basic electricity consumption data as well as the EVs' travel behavior in Beijing, this paper presents the optimal electricity price for achieving an ideal grid load fluctuation, under the scenario of V2G arbitrage considering EV battery degradation and energy loss costs.

- (1) This paper presents a multi-parameter coupled model to quantify the costs associated with EV battery degradation and energy loss. The model considers the charging and discharging characteristics of EVs and incorporates these costs into the revenue and expenditure of charging and discharging.
- (2) This study proposes an electricity pricing strategy to minimize grid load fluctuations while aligning with users' economic interests. The strategy dynamically adjusts the electricity price based on optimized load results, influencing users' charging and discharging decisions to stabilize the grid load. Under 30% V2G, the relative fluctuation of the load is reduced from 31.81% to 5.19%, which shows that electricity price adjustments can effectively reduce load fluctuations and enhance grid stability.
- (3) This study explores the effects of extended battery lifespan. With the same optimal electricity price, as the average life degradation coefficient of the EV battery decreases from CNY 0.608 to CNY 0.345, the total cost of battery degradation and energy loss for EV cluster decreases by 49.2%, and the previously optimized price remains applicable.
- (4) As the V2G participation ratios increase, the peak–valley difference of the optimal electricity price needs to decrease to maintain load stability. When the V2G participation ratio rises from 30% to 50%, the peak–valley difference of the optimal electricity price drops from CNY 1.45 to CNY 0.61. However, under a fixed average electricity price, there is no significant change in the grid's net revenue before and after price adjustments, indicating that the proposed electricity pricing adjustment strategy can effectively accommodate the increase in V2G participation.

Author Contributions: Conceptualization, Y.L. and J.D.; Methodology, C.X., P.G. and Z.W.; Validation, P.G.; Investigation, K.W.; Resources, P.G., Z.W. and J.D.; Data curation, K.W., C.X. and Z.W.; Writing—original draft, K.W.; Writing—review & editing, Y.L.; Visualization, K.W. and C.X.; Project administration, Y.L. and J.D.; Funding acquisition, Y.L. and J.D. All authors have read and agreed to the published version of the manuscript.

Funding: This research was funded by the National Key Research and Development Program of China, grant number [2022YFE0207700].

Data Availability Statement: The original contributions presented in the study are included in the article, further inquiries can be directed to the corresponding author.

Conflicts of Interest: Authors Peng Guo and Zhenlin Wu were employed by the company Shanghai Qiyuan Green Power Technology Co., Ltd. The remaining authors declare that the research was conducted in the absence of any commercial or financial relationships that could be construed as a potential conflict of interest.

References

1. Li, Y.; Wei, Y.; Zhu, F.; Du, J.; Zhao, Z.; Ouyang, M. The path enabling storage of renewable energy toward carbon neutralization in China. *eTransportation* **2023**, *26*, 100226. [[CrossRef](#)]
2. Liu, X.; Plötz, P.; Yeh, S.; Liu, Z.; Liu, X.C.; Ma, X. Transforming public transport depots into profitable energy hubs. *Nat. Energy* **2024**, *9*, 1206–1219. [[CrossRef](#)]
3. Li, Y.; Zhu, F.; Li, L.; Ouyang, M. Electrifying heavy-duty truck through battery swapping. *Joule* **2024**, *8*, 1556–1561. [[CrossRef](#)]
4. Powell, S.; Cezar, G.V.; Min, L.; Azevedo, I.M.L.; Rajagopal, R. Charging infrastructure access and operation to reduce the grid impacts of deep electric vehicle adoption. *Nat. Energy* **2022**, *7*, 932–945. [[CrossRef](#)]

5. Qin, Y.; Chen, X.; Tomaszewska, A.; Chen, H.; Wei, Y.; Zhu, H.; Li, Y.; Cui, Z.; Huang, J.; Du, J.; et al. Lithium-ion batteries under pulsed current operation to stabilize future grids. *Cell Rep. Phys. Sci.* **2022**, *3*, 100708. [[CrossRef](#)]
6. Liu, R.; He, G.; Wang, X.; Mallapragada, D.; Zhao, H.; Shao-Horn, Y.; Jiang, B. A cross-scale framework for evaluating flexibility values of battery and fuel cell electric vehicles. *Nat. Commun.* **2024**, *15*, 280. [[CrossRef](#)] [[PubMed](#)]
7. Heider, A.; Moors, F.; Hug, G. The Influence of Smart Charging and V2G on the Flexibility Potential and Grid Expansion Needs of German Distribution Grids. In Proceedings of the 2023 International Conference on Smart Energy Systems and Technologies (SEST 2023), Mugla, Turkey, 4–6 September 2023.
8. Li, Y.; Wang, K.; Xu, C.; Wu, Y.; Li, L.; Zheng, Y.; Yang, S.; Wang, H.; Ouyang, M. The potentials of vehicle-grid integration on peak shaving of a community considering random behavior of aggregated vehicles. *Next Energy* **2024**, *7*, 100233. [[CrossRef](#)]
9. Geng, J.; Bai, B.; Hao, H.; Sun, X.; Liu, M.; Liu, Z.; Zhao, F. Assessment of vehicle-side costs and profits of providing vehicle-to-grid services. *eTransportation* **2024**, *19*, 100303. [[CrossRef](#)]
10. Attou, N.; Zidi, S.A.; Hadjeri, S.; Khatir, M. Improved peak shaving and valley filling using V2G technology in grid connected Microgrid. In Proceedings of the 2021 3rd International Conference on Transportation and Smart Technologies (TST 2021), Tangier, Morocco, 27–28 May 2021.
11. Gong, J.; Wasylowski, D.; Figgener, J.; Bihm, S.; Rücker, F.; Ringbeck, F.; Sauer, D.U. Quantifying the impact of V2X operation on electric vehicle battery degradation: An experimental evaluation. *eTransportation* **2024**, *20*, 100316. [[CrossRef](#)]
12. Schwenk, K.; Meisenbacher, S.; Briegel, B.; Harr, T.; Hagenmeyer, V.; Mikut, R. Integrating Battery Aging in the Optimization for Bidirectional Charging of Electric Vehicles. *IEEE Trans. Smart Grid* **2021**, *12*, 5135–5145. [[CrossRef](#)]
13. Dubarry, M.; Devie, A.; McKenzie, K. Durability and reliability of electric vehicle batteries under electric utility grid operations: Bidirectional charging impact analysis. *J. Power Sources* **2017**, *358*, 39–49. [[CrossRef](#)]
14. Petit, M.; Prada, E.; Sauvant-Moynot, V. Development of an empirical aging model for Li-ion batteries and application to assess the impact of Vehicle-to-Grid strategies on battery lifetime. *Appl. Energy* **2016**, *172*, 398–407. [[CrossRef](#)]
15. Jafari, M.; Gauchia, A.; Zhao, S.; Zhang, K.; Gauchia, L. Electric Vehicle Battery Cycle Aging Evaluation in Real-World Daily Driving and Vehicle-to-Grid Services. *IEEE Trans. Transp. Electrif.* **2017**, *4*, 122–134. [[CrossRef](#)]
16. Carmeli, M.S.; Toscani, N.; Mauri, M. Electrothermal Aging Model of Li-Ion Batteries for Vehicle-to-Grid Services Evaluation. *Electronics* **2022**, *11*, 1043. [[CrossRef](#)]
17. Li, Y.; Feng, X.; Ren, D.; Ouyang, M.; Lu, L.; Han, X. Thermal Runaway Triggered by Plated Lithium on the Anode after Fast Charging. *ACS Appl. Mater. Interfaces* **2019**, *11*, 46839–46850. [[CrossRef](#)]
18. Cao, Y.; Li, D.; Zhang, Y.; Chen, X. Joint Optimization of Delay-Tolerant Autonomous Electric Vehicles Charge Scheduling and Station Battery Degradation. *IEEE Internet Things J.* **2020**, *7*, 8590–8599. [[CrossRef](#)]
19. Liu, L.; Liu, T.; Zhang, T.; Liu, J. Orderly Charging and Discharging Strategy Optimization for Electric Vehicles Considering Dynamic Battery-wear Model. *Autom. Electr. Power Syst.* **2016**, *40*, 83–90.
20. Zhang, Q.; Deng, X.; Yue, H.; Sun, T.; Liu, Z. Coordinated Optimization Strategy of Electric Vehicle Cluster Participating in Energy and Frequency Regulation Markets Considering Battery Lifetime Degradation. *Diangong Jishu Xuebao/Trans. China Electrotech. Soc.* **2022**, *37*, 72–81.
21. Todeschini, F.; Onori, S.; Rizzoni, G. An experimentally validated capacity degradation model for Li-ion batteries in PHEVs applications. *IFAC* **2012**, *45*, 456–461. [[CrossRef](#)]
22. Guo, N.; Peng, Z.; Huo, W.; Li, Y.; Liu, S.; Kang, L.; Wu, X.; Dai, L.; Wang, L.; Jun, S.C.; et al. Stabilizing Zn Metal Anode Through Regulation of Zn Ion Transfer and Interfacial Behavior with a Fast Ion Conductor Protective Layer. *Small* **2023**, *19*, 2303963. [[CrossRef](#)]
23. Ye, L.; Qi, S.; Cheng, T.; Jiang, Y.; Feng, Z.; Wang, M.; Liu, Y.; Dai, L.; Wang, L.; He, Z. Vanadium Redox Flow Battery: Review and Perspective of 3D Electrodes. *ACS Nano* **2024**, *18*, 18852–18869. [[CrossRef](#)] [[PubMed](#)]
24. Zahid, M.; Ahmed, F.; Javaid, N.; Abbasi, R.A.; Zainab Kazmi, H.S.; Javaid, A.; Bilal, M.; Akbar, M.; Ilahi, M. Electricity price and load forecasting using enhanced convolutional neural network and enhanced support vector regression in smart grids. *Electronics* **2019**, *8*, 122. [[CrossRef](#)]
25. Das, S.; Thakur, P.; Singh, A.K.; Singh, S.N. Optimal management of vehicle-to-grid and grid-to-vehicle strategies for load profile improvement in distribution system. *J. Energy Storage* **2022**, *49*, 104068. [[CrossRef](#)]
26. Yang, S.Y.; Woo, J.R.; Lee, W. Assessing optimized time-of-use pricing for electric vehicle charging in deep vehicle-grid integration system. *Energy Econ.* **2024**, *138*, 107852. [[CrossRef](#)]
27. Li, M. Study on Interactive Strategies between Vehicles and Grid Based on Game Theory. Master’s thesis, East China Jiaotong University, Nanchang, China, 2017.
28. Zeng, Q. Research on the Interactive Strategy of Vehicle Network Based on Dynamic Game. Master’s thesis, East China Jiaotong University, Nanchang, China, 2018.
29. Li, Z. Research on the Interactive Strategy of Electric Vehicles and Grid Based on Evolutionary Game. Master’s Thesis, East China Jiaotong University, Nanchang, China, 2019.

30. Cheng, H.; Li, Z.; Wang, X.; Zen, H.; Zhang, Y.; Kang, C.; Xin, J. Research on Two-Way Interactive Strategy of Electric Vehicle and Power Grid Based on Evolutionary Game. *Electr. Power* **2019**, *52*, 40–46.
31. Wu, J. Operation Optimization of Electric Vehicle Aggregator Considering the Participants' Behaviors. Ph.D. Thesis, Nanjing University of Science & Technology, Nanjing, China, 2019.
32. Kocer, B.; Turkyilmaz, I.; Poyrazoglu, G. Optimal Vehicle-to-Grid Controller for Energy Arbitrage and Frequency Regulation Markets. In Proceedings of the 2021 3rd Global Power, Energy and Communication Conference (GPECOM 2021), Virtual Conference, Antalya, Turkey, 5–8 October 2021.
33. Beijing Transport Institute. *Beijing Transport Development Annual Report*; Beijing Transport Institute: Beijing, China, 2016.
34. The Average Population Per Household in Beijing is 2.31 People. Guangming Net 2021. Available online: <https://m.gmw.cn/baijia/2021-05/19/1302305269.html> (accessed on 13 February 2025).
35. Outline of the 14th Five Year Plan for National Economic and Social Development and Long Range Objectives by 2035 of Beijing Municipality. Beijing Municipal Development and Reform Commission 2021. Available online: <https://www.ndrc.gov.cn/fggz/fzzlgh/dffzgh/202103/P020210331517775703990.pdf> (accessed on 13 February 2025).
36. Cui, Y. Research on Load Characteristics of Residential Buildings in Beijing Area and Application of Intelligent Network Energy Meter System, Selecting Representative Buildings in Beijing Area. *Electrotech Appl.* **2014**, *33*, 36–39.
37. Das, R.; Wang, Y.; Putrus, G.; Kotter, R.; Marzband, M.; Herteleer, B.; Warmerdam, J. Multi-objective techno-economic-environmental optimisation of electric vehicle for energy services. *Appl. Energy* **2020**, *257*, 113965. [CrossRef]
38. Birk, C.R.; Roberts, M.R.; McTurk, E.; Bruce, P.G.; Howey, D.A. Degradation diagnostics for lithium ion cells. *J. Power Sources* **2017**, *341*, 373–386. [CrossRef]
39. Schatz, E.; Khaligh, A.; Rasmussen, P.O. Influence of battery/ultracapacitor energy-storage sizing on battery lifetime in a fuel cell hybrid electric vehicle. *IEEE Trans. Veh. Technol.* **2009**, *58*, 3882–3891. [CrossRef]
40. Naumann, M.; Spangler, F.; Jossen, A. Analysis and modeling of cycle aging of a commercial LiFePO₄/graphite cell. *J. Power Sources* **2020**, *451*, 227666. [CrossRef]
41. How to Calculate the Overload of a Transformer. ZX-ELE 2024. Available online: <https://www.zx-ele.com/new/how-to-calculate-the-overload-of-a-transformer> (accessed on 13 February 2025).
42. Muthukrishnan, R.; Rohini, R. LASSO: A feature selection technique in predictive modeling for machine learning. In Proceedings of the 2016 IEEE International Conference on Advances in Computer Applications (ICACA2016), Coimbatore, India, 24 October 2016.
43. Over 30 Million New Energy Vehicles are Running on the Roads of China. Guangming Net 2025. Available online: https://m.gmw.cn/2025-01/19/content_1303951233.htm (accessed on 13 February 2025).

Disclaimer/Publisher's Note: The statements, opinions and data contained in all publications are solely those of the individual author(s) and contributor(s) and not of MDPI and/or the editor(s). MDPI and/or the editor(s) disclaim responsibility for any injury to people or property resulting from any ideas, methods, instructions or products referred to in the content.